Journal of Medicinal Chemistry

Article

pubs.acs.org/jmc

Dual Inhibitors for Aspartic Proteases HIV-1 PR and Renin: Advancements in AIDS–Hypertension–Diabetes Linkage via Molecular Dynamics, Inhibition Assays, and Binding Free Energy Calculations

Haralambos Tzoupis,[†,‡] Georgios Leonis,*[,†] Grigorios Megariotis,[†,§] Claudiu T. Supuran,[∥] Thomas Mavromoustakos,[‡] and Manthos G. Papadopoulos*[,†]

[†]Institute of Organic and Pharmaceutical Chemistry, National Hellenic Research Foundation, 48 Vas. Constantinou Avenue, Athens 11635, Greece

[‡]Department of Chemistry, National and Kapodistrian University of Athens, Panepistimioupolis Zographou, Athens 15771, Greece

[§]School of Chemical Engineering, National Technical University of Athens, 9 Heroon Polytechniou Street, Athens 15780, Greece

[∥]Department of Chemistry, University of Florence, Via della Lastruccia 3, Rm 18, 50019 Sesto Fiorentino (Florence), Italy

Supporting Information

ABSTRACT: Human immunodeficiency virus type 1 protease (HIV-1 PR) and renin are primary targets toward AIDS and hypertension therapies, respectively. Molecular mechanics Poisson–Boltzmann surface area (MM–PBSA) free-energy calculations and inhibition assays for canagliflozin, an antidiabetic agent verified its effective binding to both proteins (ΔG_{pred} = −9.1 kcal mol^{-1} for canagliflozin–renin; $K_{i,exp}$= 628 nM for canagliflozin–HIV-1 PR). Moreover, drugs aliskiren (a renin inhibitor) and darunavir (an HIV-1 PR inhibitor) showed high affinity for HIV-1 PR ($K_{i,exp}$= 76.5 nM) and renin ($K_{i,pred}$= 261 nM), respectively. Importantly, a high correlation was observed between experimental and predicted binding energies (r^2 = 0.92). This study suggests that canagliflozin, aliskiren, and darunavir may induce profound effects toward dual HIV-1 PR and renin inhibition. Since patients on highly active antiretroviral therapy (HAART) have a high risk of developing hypertension and diabetes, aliskiren-based or canagliflozin-based drug design against HIV-1 PR may eliminate these side-effects and also facilitate AIDS therapy.

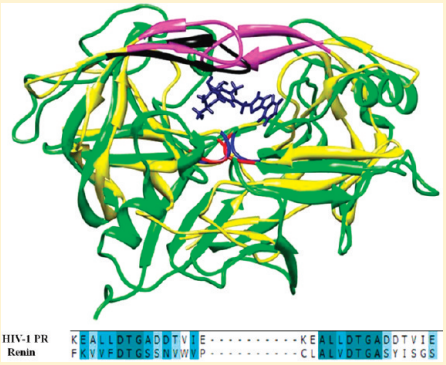

INTRODUCTION

Acquired immunodeficiency syndrome (AIDS) is an incurable and potentially fatal disease with more than 36 million people affected and over 27 million who have succumbed to it since 1981 (estim. 2009, UNAIDS).[1] It is also estimated that more than 1 billion people worldwide have developed some type of hypertension.[2] The population data suggest that both conditions present a public health challenge on a global scale. Extensive research has mapped the biochemical pathways for both diseases, and potential drug targets have been identified. Following the recognition of human immunodeficiency virus type 1 (HIV-1) as the primary cause of AIDS, the choice of HIV-1 protease (HIV-1 PR) as a target for rational drug design became apparent since HIV-1 PR plays an essential role in viral maturation.[3] Regarding the treatment of hypertension, the renin–angiotensin–aldosterone system (RAAS) is of paramount importance in regulating blood pressure.[4] Renin cleaves the amide bond between Leu10-Val11 of angiotensinogen, leading to the production of the decapeptide angiotensin I, a critical step in RAAS, since this is the rate-determining step for the entire pathway.[5−7] Angiotensin I is finally converted to the active peptide angiotensin II, which causes increase in blood pressure. Thus, inactivation of renin would inhibit the rate-limiting step and may lead to an effective therapeutic strategy against hypertension.

HIV-1 PR and renin belong to the family of aspartic proteases, a small group of proteins that share common features.[8−12] A characteristic in this family of enzymes is the presence of two aspartic acid residues at the active site, as parts of two conserved catalytic triads (Asp-Thr-Gly). The mechanism of the cleavage reaction involves proton transfer between the substrate and the aspartic acids at the catalytic site, thus leading to hydrolysis of the peptide bond in the substrate. Another common characteristic of aspartic proteases is that the catalytic center is located at the bottom of a substrate-binding cleft.[9−13] In 1991, Sharma et al. showed that viral HIV-1 PR is able to produce angiotensin I at similar levels with human renin.[14] This bioassay offered insight into the cleavage mechanism of both enzymes and supported the hypothesis that aspartic proteases have functional similarities. Furthermore, Zhang et al. used zinc ions to inhibit the function of the two

Received: February 9, 2012
Published: May 24, 2012

proteases; they observed inhibitory action, noncompetitive for renin and competitive/noncompetitive for HIV-1 PR.[15] In both cases, inhibition occurred in the same way and was pH dependent, similar to other proteins of the same family (e.g., pepsin).

HIV-1 PR possesses a symmetric structure, comprising two identical chains with 99 amino acids each. The active site consists of two catalytic regions (Asp25-Thr26-Gly27 in chain A and Asp25′-Thr26′-Gly27′ in chain B) located at the bottom of a large substrate-binding cleft.[10,11] In the outer part of the protease and directly exposed to the solvent, two glycine-rich β-hairpins or flaps (residues 45−55 and 45′−55′) cover the cleft and control the entrance of substrates into the binding cavity. Several crystallographic and NMR data, along with computational studies suggest that the flaps of the apo protein are significantly flexible and appear in equilibrium among "open," "semi-open," and "closed" states.[9−11] While most of the inhibitor-bound forms of HIV-1 PR display a "closed" configuration with stable flaps, the flaps of the free protease primarily acquire "semi-open" conformations, thus resulting in a more mobile structure.[16−18]

Renin consists of one polypeptide chain with 340 amino acids. The active site of the protease (Asp32/215, Thr33/216, and Gly34/217) is also located inside a deep pocket covered by a single loop consisting of residues in the vicinity of Ser76. Similar to the flaps of HIV-1 PR, the Ser76 loop is implicated in modulating ligand access to the cavity and appears very mobile in the apo form of renin before it stabilizes in a "closed" conformation upon binding.[19,20] The comparison of HIV-1 PR and renin structures is given in Figure 1. Alignment of the amino acid sequences around the conserved catalytic triads shows great similarity between the two enzymes. The sequence comparison revealed additional common features such as a hydrophobic area, which precedes the active site region in both proteins: Ala-Leu-Leu in HIV-1 PR and Val-Val-Phe/Ala-Leu-Val in renin. Also, according to experimental and theoretical evidence, the active site in both proteins appears to be monoprotonated.[15,21−24]

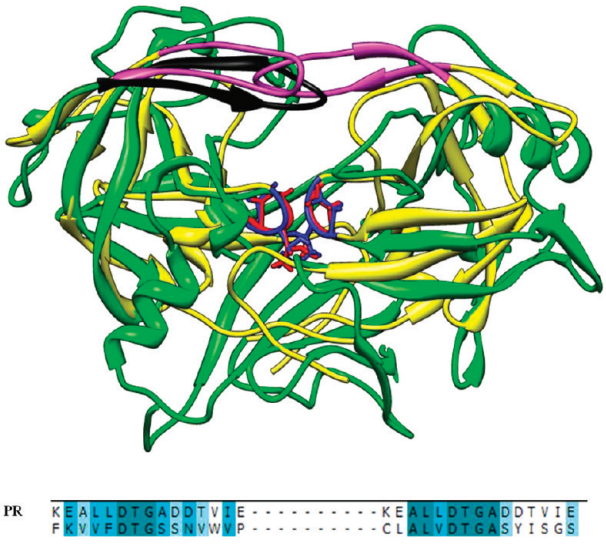

Figure 1. Top: structural alignment of HIV-1 PR (yellow) and renin (green) shows common features between proteases. The active site D-T-G of HIV-1 PR (blue) and of renin (red), along with the flap region of HIV-1 PR (purple) and of renin (black) are also highlighted. Bottom: alignment of residues in the vicinity of the catalytic triads for HIV-1 PR and renin. Dark blue, identical residues; blue, strong alignment; light blue, weak alignment; white, no alignment.

Despite the aforementioned approaches and the apparent observation that renin and HIV-1 PR share common features, there are no extensive comparisons regarding their mode of action. Combining computational methodologies with experimental data enables the search through a wide range of compounds for potential inhibitory activity against HIV-1 PR and renin. As a continuation of our studies on the binding patterns and the interactions involving HIV-1 PR[25] and renin complexes,[19] we aimed to identify similarities between proteases with respect to their binding mode and conformational properties upon binding. Smith and co-workers have proposed that the common structural and functional features of the two proteases can help toward the design of potential dual inhibitors; it was shown that compounds based on the same scaffold (e.g., pyrrolinone rings) could have inhibitory effects on both proteases.[26] Following this suggestion, an appropriately selected substance (canagliflozin), along with two commercially available drugs, darunavir and aliskiren, have been examined as potential, dual inhibitors of HIV-1 PR and renin. Canagliflozin is involved in the treatment of type 2 diabetes and as of 2010 it is still in the phase of clinical trials.[27] It was developed by Johnson and Johnson and is a C-aryl glucoside.[28] It inhibits sodium glucose cotransporter 2 (SGLT2), a 14 transmembrane protein.[29] Darunavir is the most recently FDA-approved anti-HIV drug, with a chemical structure designed to increase favorable hydrogen bonding (HB) interactions with HIV-1 PR.[30−34] It exhibits remarkable enzyme inhibitory potency (K_i = 16 pM) and antiviral activity (IC_{90} = 4.1 nM).[35] Aliskiren is the first orally active, direct renin inhibitor to be approved for the treatment of hypertension.[13] A highly potent human renin inhibitor, aliskiren has IC_{50} in the low nanomolar range (0.6 nM) and a biological half-life of ≈24 h.[36]

Molecular dynamics (MD) approaches have been applied to explore the conformational diversity of the following systems: canagliflozin−HIV-1 PR, aliskiren−HIV-1 PR, canagliflozin−renin, and darunavir−renin. Additionally, binding affinities can be quantitatively estimated by a variety of free-energy simulation techniques;[37−39] the molecular mechanics Poisson−Boltzmann surface area (MM−PBSA) method is a reliable approach to compute the absolute binding free-energy change in biomolecular systems.[40−42] This method combines molecular mechanics (MM) energies (bond, angle, torsion, van der Waals, and electrostatic terms) for the solute with the solvation free energy. The latter is calculated by solving numerically the Poisson−Boltzmann (PB) equation and approximating the nonpolar free energy with a simple surface area term. Finally, the entropic contribution may also be introduced by normal-mode analysis to estimate more accurately the total free energy.

Our rationale is summarized as follows: (a) canagliflozin has been selected as the inhibitor, which combined optimal docking scores in both HIV-1 PR and renin, (b) drugs darunavir and aliskiren have been mutually exchanged between HIV-1 PR and renin, respectively, to identify the behavior of each protein when bound to an inhibitor associated with the other protein. Discerning any differences or similarities between structural and binding patterns of the two proteases, it is possible to derive conclusions regarding the role of canagliflozin, darunavir, and aliskiren as *dual* inhibitors of HIV-1 PR and renin.

To validate our results, inhibition assays have been performed for canagliflozin−HIV-1 PR and aliskiren−HIV-1 PR complexes. Finally, the interaction between aliskiren and a

dx.doi.org/10.1021/jm300180r | J. Med. Chem. 2012, 55, 5784−5796

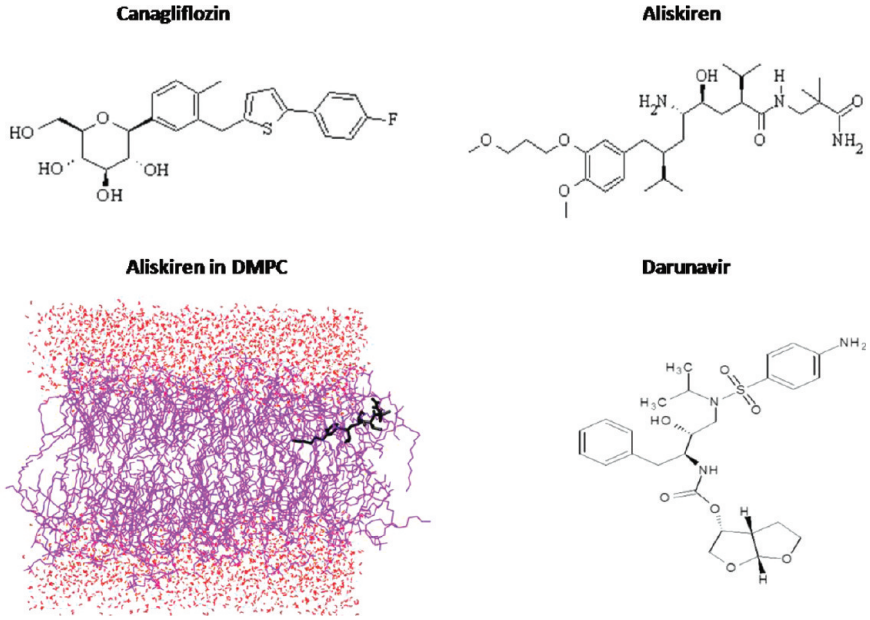

Figure 2. Compounds considered in this study. Aliskiren into DMPC bilayer is colored black.

dimyristroyl phosphatidyl choline (DMPC) bilayer was studied through long MD simulations. It is known that drugs have to cross the water−bilayer regions to exert their biological action inside the cell,[43] and according to previous pharmacokinetic studies, aliskiren exhibits sufficient membrane permeability that results in intestinal absorption.[36] Thus, we have performed calculations to test the ability of aliskiren to penetrate into DMPC bilayers and to identify dominant interactions and conformational properties of the drug in the interior of the bilayer. The three key compounds studied and aliskiren incorporation in the core of the DMPC membrane bilayer are presented in Figure 2.

The aim of this study was to test the hypothesis of whether canagliflozin, darunavir, and aliskiren may serve as dual inhibitors of HIV-1 PR and renin. Then, the linkage among AIDS, hypertension, and diabetes could be explored at the molecular level. The use of highly active antiretroviral therapy (HAART) in AIDS has decreased the mortality rate of HIV-infected patients. Clinical studies have demonstrated the relationship among lypodystrophy, hypertension, and diabetes, as well as among AIDS, hypertension, and diabetes.[44,45] According to investigations regarding the latter, HIV-positive patients who take HIV-1 PR inhibitors are more likely to develop diabetes, with the risk being three to five times greater compared to HIV-negative people.[46] This intrigued us further to test the inhibitory potency of canagliflozin against HIV-1 PR. HIV-1 PR inhibition by canagliflozin may assist AIDS treatment, and at the same time, the side-effect causing diabetes could be diminished. Also, HIV-infected patients have a higher risk of developing hypertension, especially if a protease inhibitor (PI) has been included in HAART. In a study concerning 283 patients, the prevalence of hypertension was 21% among 219 patients on HAART and 19% among 64 HAART-naïve patients.[47] In another study with 5622 participants, patients on HAART for less than two years did not deviate in developing hypertension from the general population, whereas patients continuing HAART for more than 5 years showed a significant increase in developing hypertension.[48] The implications of possible dual HIV-1 PR and renin inhibition by a single compound are direct and may help the development of new drugs that assist both anti-HIV and antihypertensive action.

METHODS

An extensive literature search through the Web of Science (Thomson ISI) platform for diverse, recently published studies (years 2010 and 2011) of enzyme inhibitors with biological activity data and with similar properties (e.g., size and molecular weight) as those of darunavir and aliskiren resulted in totally 54 compounds (Table S1, Supporting Information). All compounds were subjected to molecular docking calculations into the binding sites of HIV-1 PR and renin. Canagliflozin was selected for further MD and binding free-energy calculations in HIV-1 PR and renin complexes due to its optimal combination of docking results into both proteins. Additionally, for comparison all commercially available HIV-1 PR and renin inhibitors have been docked into the active sites of both proteins (Table S2, Supporting Information).

Our methodology included (i) a series of docking calculations for rapid selection, through a broad database of inhibitors, of the compound canagliflozin as a candidate inhibitor against both HIV-1 PR and renin; (ii) MD simulations for canagliflozin−HIV-1 PR, canagliflozin−renin, aliskiren−HIV-1 PR, and darunavir−renin complexes to compare conformational properties and dominant interactions between inhibitors and proteases; (iii) MM−PBSA calculations to estimate the binding affinities and to decompose the energetic impact on each complex; (iv) inhibition assays for canagliflozin−HIV-1 PR and aliskiren−HIV-1 PR complexes to validate our calculations; (v) MD calculations of aliskiren into DMPC bilayer to identify principal conformations and interactions between aliskiren and the bilayer; (vi) MD simulations of apo HIV-1 PR and apo renin to compare the behavior of the complexes to the unbound proteases. Combination of (ii), (iii), (iv), and (vi) enabled us to assess the suitability of specific substances as dual inhibitors of HIV-1 PR and renin.

Molecular Docking Calculations. Docking scores for all systems have been calculated using the DOCK 6.4 suite.[49,50] Ligands were prepared with the UCSF Chimera 1.5.2 module,[51] and their charges have been calculated according to the AM1 atomic charge methodology with simple additive bond charge corrections (AM1-BCC).[52,53] The DockPrep function of Chimera was used to prepare the two proteins. The molecular surface of the proteins was generated using the DMS tool with a probe radius of 1.4 Å. The sphgen module[54] of

dx.doi.org/10.1021/jm300180r | J. Med. Chem. 2012, 55, 5784−5796

DOCK has been employed to create the sphere centers that fill the six-residue active site of HIV-1 PR and renin. Subsequently, the grid module[55] has been used to generate the scoring grid using a box of 25 Å × 25 Å × 25 Å. Contribution to the energy score was calculated for a maximum distance of 10 Å between two atoms, and an all-atom model was used for nonpolar hydrogen atoms. Ligands were considered as flexible units, whereas proteins were kept rigid during docking. The number of maximum orientations to be cycled through was set to 10^7.

Molecular Dynamics Simulations in Water. All-atom, unrestrained MD simulations in explicit solvent have been carried out for the four complexes using the SANDER module under the AMBER 11 software package.[56] The high resolution protein structures were obtained from the Brookhaven Protein Databank (PDB codes: 2IEN and 2V0Z for darunavir−HIV-1 PR and aliskiren−renin complexes, respectively).[57] Crystal water molecules and ligands were removed from the crystal structures prior the addition of missing hydrogen atoms, using the tLEaP module of AMBER. After removing the inhibitors, the apo structures of 2IEN and 2V0Z were also subjected to MD analysis, to account for the behavior of the unbound proteases. Aliskiren-bound HIV-1 PR and darunavir-bound renin were constructed after exchanging inhibitors between 2IEN and 2V0Z; canagliflozin was also docked into the binding cavities of HIV-1 PR and renin after removing darunavir and aliskiren from the crystal structures 2IEN and 2V0Z, respectively. The force field ff99SB was used to represent the behavior of the proteins.[58] Ligand structures were constructed with the ANTECHAMBER module (using the GAFF force field with AM1-BCC charges).[59] Systems were neutralized with tLEaP by adding 6 Cl^- and 7 Na^+ counterions to HIV-1 PR complexes and renin complexes, respectively. Each system was solvated using the TIP3P water model[60] in truncated octahedral periodic boundary conditions, with a cutoff distance of 10 Å. Long range electrostatic interactions were calculated using the particle mesh Ewald (PME) method.[61] According to the aforementioned studies, both HIV-1 PR and renin were considered monoprotonated.[21−24] The starting step was the minimization of the systems over 5000 steps. For the first 2500 steps, the steepest descent method was used, while for the next 2500 steps a conjugate gradient algorithm was employed. The next procedure involved the gentle heating of each complex under constant volume, over 50 ps with the gradual increase of the temperature from 0 to 300 K (time step: 1 fs). An 100 ps constant-pressure equilibration followed, to observe the gradual increase of the density, which converged after ≈30 ps. Subsequently, a 20 ns−long MD production simulation in constant pressure was performed for each system (canagliflozin−HIV-1 PR, canagliflozin−renin, darunavir−renin, aliskiren−HIV-1 PR, apo HIV-1 PR, and apo renin) using a Langevin dynamics temperature scaling with a collision frequency of 2 ps^{-1}.[62] During the MD simulations, all bonds involving hydrogen atoms were constrained to their equilibrium distance,[63] thus allowing for a 2 fs time step to be used. Further analysis (distance, rmsd, fluctuations, and HB calculations) was performed on the resulting trajectories with the ptraj module under AMBER. A 3.5 Å donor−acceptor distance cutoff and a cutoff of 120° for the donor−hydrogen−acceptor angle have been used to define HB interactions.

Computational details on the MD simulations in aliskiren−DMPC system are provided in the Supporting Information.

MM−PBSA Calculations. MM−PBSA is an end point method that involves calculations of free energy differences between two states. The partition of the binding free energy into contributions allows for a valuable insight into the complex process of association.[64] For each ligand−protein system, the binding free energy change (ΔG_{bind}) accompanies the binding process:

$$\text{protein} + \text{ligand} \rightarrow \text{complex}$$

The procedure was applied by considering 2500 snapshots of the complexes that did not contain any water molecules or counterions. For every snapshot, the binding free energy for the complex is calculated using the following equation:

$$\Delta G_{bind} = G_{complex} - (G_{protein} + G_{ligand}) \quad (1)$$

where ΔG_{bind} is the total binding free energy, $G_{complex}$, $G_{protein}$, and G_{ligand} are the energies for the complex, the protein (HIV-1 PR, renin) and the ligand (canagliflozin, darunavir, aliskiren), respectively. The binding energy can be also expressed as a combination of enthalpic and entropic contributions:

$$\Delta G_{bind} = \Delta H - T\Delta S \quad (2)$$

The enthalpy of binding is given by the following equation:

$$\Delta H = \Delta E_{MM} + \Delta G_{sol} \quad (3)$$

where ΔE_{MM} defines the interaction energy between the protein and the ligand computed with the molecular mechanics method, and ΔG_{sol} is the solvation free energy.

ΔE_{MM} is further divided into

$$\Delta E_{MM} = \Delta E_{elec} + \Delta E_{vdW} \quad (4)$$

ΔE_{elec} is the electrostatic interaction energy, and ΔE_{vdW} is the van der Waals interaction energy. For the calculation of these two terms, no cutoff point was applied. Furthermore, the solvation energy (eq 3) is defined by the combination of electrostatic (ΔG_{PB}) and nonpolar (ΔG_{NP}) contributions:

$$\Delta G_{sol} = \Delta G_{PB} + \Delta G_{NP} \quad (5)$$

The electrostatic (ΔG_{PB}) energy is approximated by the Poisson−Boltzmann (PB) method[64] using the PBSA module of AMBER, and the hydrophobic contribution to solvation (ΔG_{NP}) is determined via calculation of the solvent-accessible surface area (SASA):

$$\Delta G_{NP} = \gamma \text{SASA} + \beta \quad (6)$$

for the surface tension γ and for the offset β, we have considered the standard values of 0.00542 kcal mol^{-1} $Å^{-2}$ and 0.92 kcal mol^{-1}, respectively. ΔG_{NP} was computed via eq 6, with the linear combinations of pairwise overlaps (LCPO) method.[65] A probe radius of 1.4 Å has been also used for the SASA calculation.

Following recent studies on the optimal performance of MM−PBSA for hydrophobic systems, the values for the dielectric constant of the solvent and the solute were set to 80.0 and 1.0, respectively.[66] The entropic contribution (eq 2) was calculated using the nmode module of AMBER, over 200 snapshots to save computational time. The performance of MM−PBSA has been recently evaluated.[66] Six different protein systems have been tested as substrates for 59 ligands. Various factors, such as the length of the MD simulation and the values of the solute dielectric constant have been considered to affect the quality of the results. Particularly, the importance of the conformational entropy was emphasized, as well as the adequacy of MM−PBSA to reliably calculate binding free energies. Instead of modeling the water environment by explicit simulations, MM−PBSA discards the water molecules and uses a parametrized implicit water model (PB). Sometimes, this may be a disadvantage that accounts for differences between predictions and experimental results. However, the LCPO method for estimating the hydrophobic contribution shows sufficient performance even for hydrophobic systems, such as the binding cavities of HIV-1 PR and renin, and it is satisfactorily reproducing the experimental results.[67]

Clustering. Clustering calculations for canagliflozin into HIV-1 PR and renin have been performed with a hierarchical approach from the MOIL-View 10.0 program.[68] As the distance metric for clustering, a 3.0 Å rmsd cutoff was introduced to classify 10000 conformations. The representative structures produced by the clustering were used for further analysis.

HIV-1 PR Inhibition Assays. Aliskiren hemifumarate was obtained from the company SAS ALSACHIM−BIOPARC and canagliflozin from ShangHai Biochempartner Co., Ltd. HIV-1 PR inhibition was performed by a spectrophotometric assay using the chromogenic peptide substrate LysAlaArgValNle·NphGluAlaNle-NH_2 as described by Weber et al.[69] Typically, 8−10 pmol of HIV-1 PR (a recombinant enzyme from Sigma−Aldrich, Milan, Italy) was added to 1 mL of 0.1 M sodium acetate buffer, (pH 4.7), 0.3 M NaCl, and 4 mM EDTA, containing substrate at a concentration near the K_m of the enzyme

dx.doi.org/10.1021/jm300180r | J. Med. Chem. 2012, 55, 5784−5796

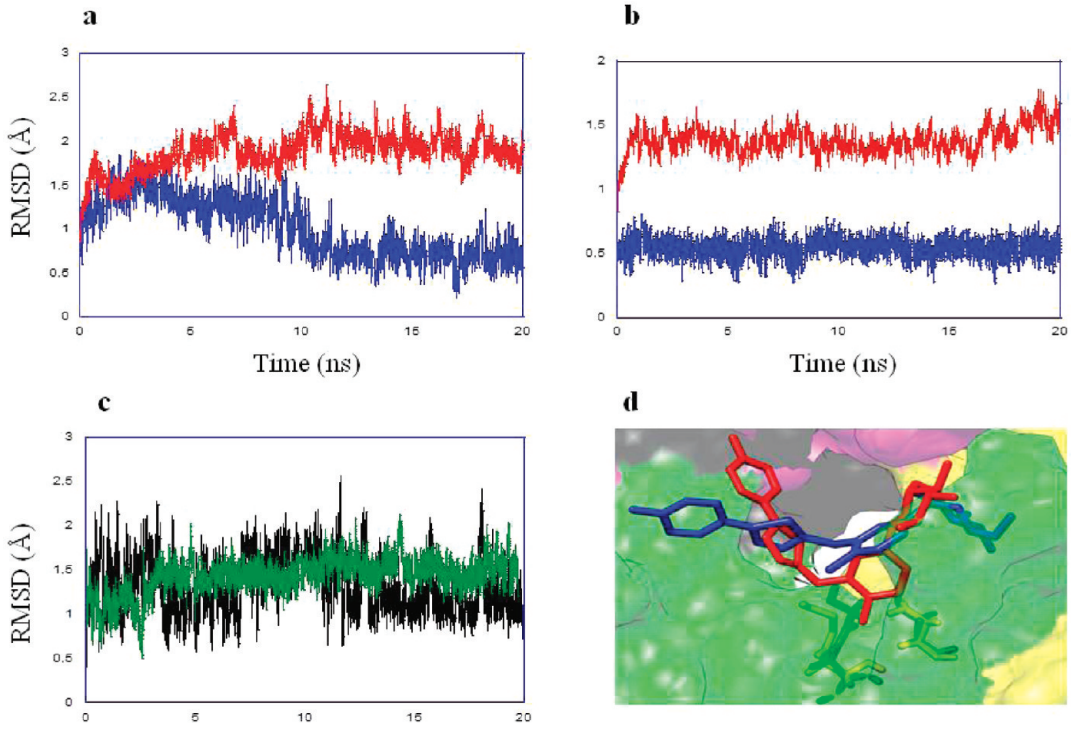

Figure 3. Rmsd of (a) HIV-1 PR and (b) renin, in complexes with canagliflozin, starting from the structures obtained after equilibration and overlapped on the corresponding crystal structures. Superpositions of different Cα atoms are displayed: all protease residues are designated in red and active site residues in blue; (c) Rmsd for all atoms of canagliflozin in HIV-1 PR (black) and renin (green); (d) representative conformations of canagliflozin in HIV-1 PR (blue) and renin (red). The binding cavities and flap regions of the proteases are represented as surfaces, and the coloring is according to Figure 1. The active sites of HIV-1 PR (yellow) and renin (green) are also shown.

(which is of 15 μM)[69] and various concentrations of the inhibitor dissolved in DMSO (from 0.1 mM to 0.01 nM, in consecutive 10-fold dilutions). Most inhibition assays were run working at 15 μM concentration of substrate, which coincided with the half maximal activity of the enzyme. As all protease inhibitors (PIs) have a free OH moiety, aliskiren is a competitive inhibitor with the chromogenic substrate used in the assay. The final concentrations of DMSO were kept below 2.5% (v/v). Substrate hydrolysis was followed as a decrease in absorbance at 305 nm using a Cary 3-500 UV−vis spectrophotometer (Cambridge, UK). The temperature of the experiments was kept at 293 K. The HIV-1 PR remained stable over the whole reaction time. Inhibition data were analyzed using the equation for competitive inhibition according to Williams and Morrison.[70] The IC_{50} values were converted to K_i using the Cheng−Prusoff equation:[71]

$$K_i = IC_{50}/(1 + [S]/K_m) \quad (7)$$

where [S] = substrate concentration; K_m = the concentration of substrate at which the enzyme activity is at half maximal. In this particular case, [S] = K_m and $K_i = IC_{50}/2$. As standard in the inhibition assay was used darunavir, which provided a K_i of 0.5 nM.

RESULTS AND DISCUSSION

In this section, structural properties and principal interactions involving complexes of HIV-1 PR and renin are investigated in detail. To complement our study, binding energies and the behavior of aliskiren in the aqueous DMPC bilayer have been estimated as well. Simulation details of the aliskiren−DMPC system and relevant discussion are provided in the Supporting Information.

Conformational Properties of HIV-1 PR and Renin in Complexes with Canagliflozin. The replacement of crystal inhibitors in each protein by canagliflozin resulted in a structural change of the proteases upon the beginning of the simulation. Despite the initial structural rearrangement, the trajectories eventually converged toward a stable state as indicated by the Cα-based rmsd values, with respect to their crystal structures (Figure 3a and b, red). Conformational changes were observed in the HIV-1 PR complex during the first half of the simulation, which resulted in a relatively stable trajectory after 10 ns, while the renin structure did not present major variations during the simulation. The final rms change induced in HIV-1 PR appeared slightly more profound than the one induced in renin (average rmsd ≈2 Å for HIV-1 PR, average rmsd ≈1.5 Å for renin), and HIV-1 PR displayed greater mobility than renin. These may be indications of less efficient binding of canagliflozin to HIV-1 PR than to renin, a possibility to be investigated during the course of this work. As expected, the active site region of the two proteases presented less variation, with average rmsd values for both systems ≈0.6 Å (Figure 3a and b, blue). Interestingly, the replacement of darunavir with canagliflozin in HIV-1 PR resulted in an immediate rms difference ≈1.5 Å for the active site of the protease, thus denoting an unfavorable rearrangement of the binding cavity upon insertion of the new substrate. After analyzing the contribution of individual active site residues to the total rms deviation of the active site, it was found that this rearrangement was mainly attributed to the increased flexibility of Asp25/25′, which reflected upon the whole structure of HIV-1 PR. However, after ≈10 ns a structural change in the active site region resulted in a more favorable positioning of canagliflozin into the binding pocket, and the active site residues acquired conformations that resembled their darunavir-bound structure.

Compared to the apo form of renin, we observed that the canagliflozin−renin complex displayed structural characteristics

dx.doi.org/10.1021/jm300180r | J. Med. Chem. 2012, 55, 5784−5796

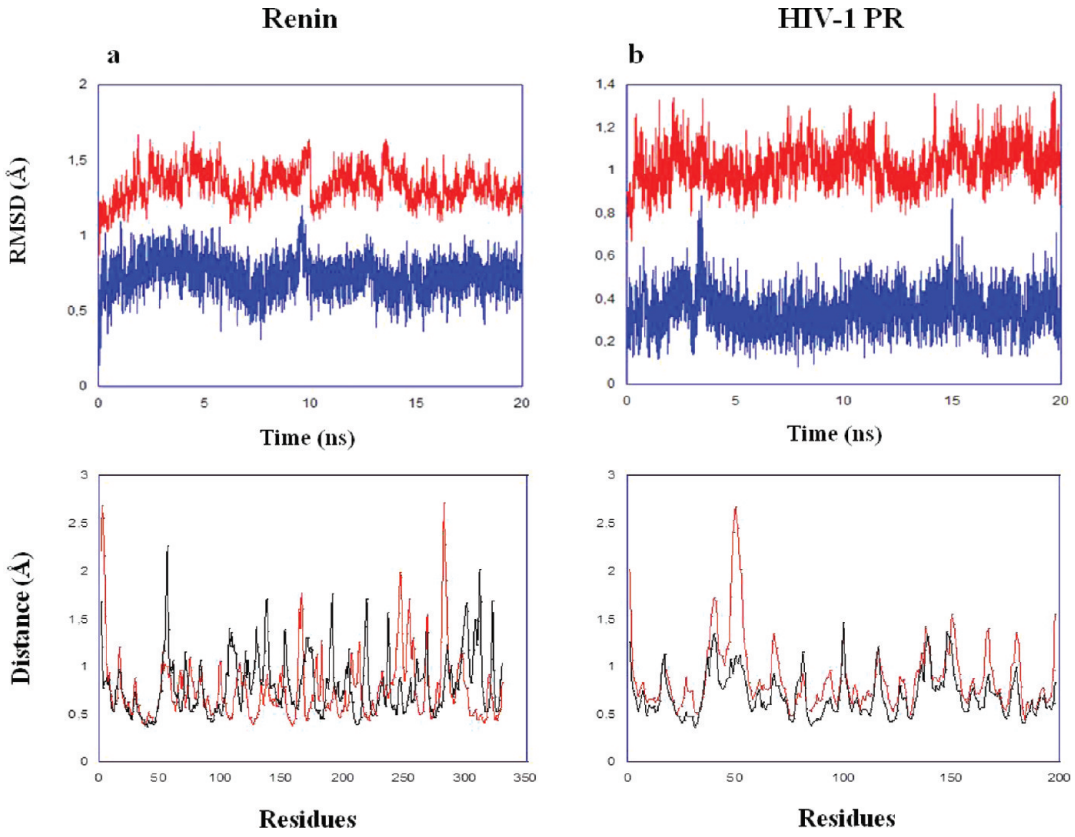

Figure 4. (a) Darunavir–renin and (b) Aliskiren–HIV-1 PR complexes: Cα-rmsd of protease residues (red) and of active site residues (blue); Cα atomic fluctuations for protease residues in (c) canagliflozin–renin (red) and darunavir–renin (black); (d) canagliflozin–HIV-1 PR (red) and aliskiren–HIV-1 PR (black).

that accompany binding (Figure S1, Supporting Information): unbound renin appeared more flexible (due to the increased mobility of the flap) and with higher rms deviations, reaching values up to 2.7 Å. Similar to canagliflozin-bound renin, the structure of the active site remained practically stable in the apo form, but it showed greater deviation from the crystal structure than the bound form. This implied that the active site may interact with canagliflozin toward effective binding. In particular, analysis of the contribution of individual active site residues to the total rmsd of the active site revealed that Gly217 appears practically unchangeable, thus suggesting that it may play an important role in canagliflozin binding.

Several experimental and computational studies have associated effective binding in aspartic protein complexes with a so-called "shift" of the flaps toward the active site.[10,17−19] To investigate this behavior in our systems, we have monitored the active site–flap distance during the simulation, for both complexes. Canagliflozin appeared less effectively trapped into HIV-1 PR than into renin since the one flap (Ile50) in HIV-1 PR is mobile enough to fluctuate in distances ranging from 16 Å to 26 Å away from the Asp25 active site (Figure S2a, Supporting Information). However, the flap (Ser76)–active site (Asp32) distance for canagliflozin–renin complex was less fluctuating, thus denoting a more stable structure of the binding cavity that may implicate a tighter binding (Figure S2b, Supporting Information). Despite the more fluctuating active site–flap distance distribution in HIV-1 PR complex, a tendency for the distance to decline over time was frequently observed in both complexes, so that an indication of effective binding as expressed by the aforementioned shift was evident. These findings suggest that even though both systems showed patterns that accompany effective binding, the canagliflozin–renin complex has more pronounced binding characteristics than the complex of HIV-1 PR with canagliflozin. Finally, another observation, which supports the enhanced binding characteristics of canagliflozin in renin was the increased stability of the compound inside renin cavity (Figure 3c).

Clustering calculations in canagliflozin–HIV-1 PR and canagliflozin–renin complexes revealed the dominant conformations of the substrate into both cavities (Figure 3d). It was shown that canagliflozin was able to bind to the two targets in different conformations: it adopted an extended conformation when bound to HIV-1 PR, whereas the binding cavity of renin induced a rather bent structure to canagliflozin. It could be assumed that this flexibility may also be responsible for canagliflozin acting as a dual inhibitor of HIV-1 PR and renin.

Conformational Properties of Darunavir–Renin Complex. Following the structural investigation of canagliflozin into HIV-1 and renin proteases, an analogous study on the darunavir–renin complex has been attempted. Considering the structural stability of the complex, it was observed that the trajectory converged smoothly after a period of ≈10 ns. Darunavir is a strong HIV-1 PR inhibitor; however, the presence of the drug induced very minor changes to renin (as expressed by the rmsd values in Figure 4a), thus indicating the possibility of effective renin inhibition as well. A similar behavior was observed for the rms deviations of the active site of renin, where the initial conformational change rapidly converged to low values around 0.7 Å. Another structural change at 7–10 ns may have resulted from an HB

dx.doi.org/10.1021/jm300180r | J. Med. Chem. 2012, 55, 5784−5796

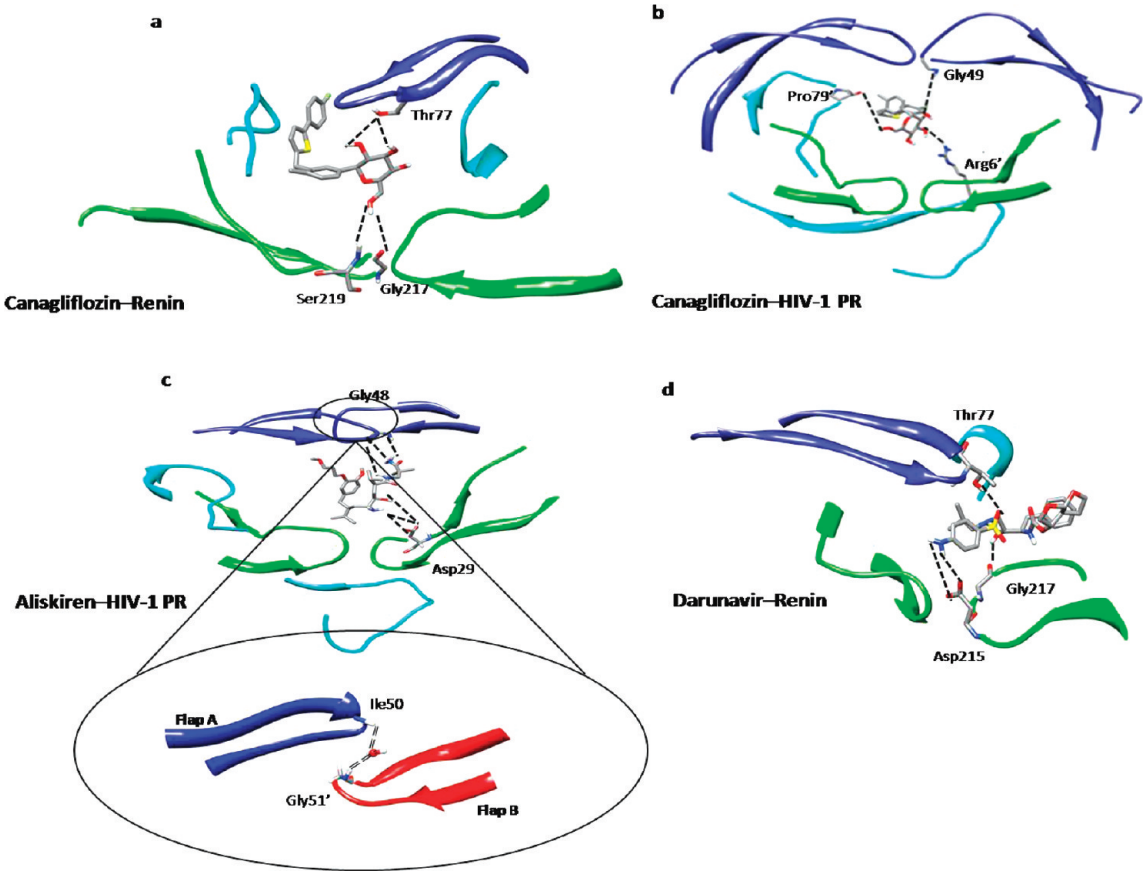

Figure 5. Principal hydrogen bonding interactions between (a) canagliflozin and renin; (b) canagliflozin and HIV-1 PR; (c) aliskiren and HIV-1 PR; a hydrogen bond between HIV-1 PR flaps is facilitated by a water molecule (inlaid schematic); and (d) darunavir and renin.

rearrangement between the inhibitor and the active site of renin. A flap shift toward the active site induced by the presence of darunavir inside renin was also observed after 6 ns and eventually resulted in a relatively stable flap−active site distance (Figure S2c, Supporting Information).

Additionally, rms fluctuations for darunavir in renin provided support of effective binding since the inhibitor appeared significantly stable inside the cavity. In Figure S3a (Supporting Information), the converged rms values for darunavir into renin are given.

Conformational Properties of Aliskiren−HIV-1 PR Complex. The last part of the conformational study involved the elucidation of features induced by the presence of aliskiren inside HIV-1 PR. Similarly to darunavir's behavior in renin, aliskiren displayed promising results when bound to HIV-1 PR: the protease underwent very minor structural changes upon aliskiren binding, indicating the possibility of significant HIV-1 PR inhibition. Relevant conformational features are presented in Figure 4b. Rmsd values for HIV-1 PR were even lower and less fluctuating than the corresponding values of HIV-1 PR when bound to canagliflozin.

Further support was provided by the observation of a stabilized aliskiren structure inside HIV-1 PR. The average displacement of the inhibitor was 1.7 Å, being tightly settled close to the binding site (Figure S3b, Supporting Information). Flap−active site distance in aliskiren−HIV-1 PR was initiated at ≈14 Å and gradually increased during the first 5 ns of the simulation to eventually converge to an average value of 16.5 Å (Figure S2d, Supporting Information). The structure of the complex remained stable during the simulation with the flaps covering aliskiren in a tight conformation.

Structural Flexibility of HIV-1 PR and Renin. Cα atomic fluctuation calculations for each residue of HIV-1 PR and renin upon binding to canagliflozin, darunavir, or aliskiren provided additional information on the ability of each ligand to induce effective binding. Canagliflozin induced a slightly higher flexibility to HIV-1 PR compared to aliskiren: especially, flapA (Ile50) appeared increasingly mobile (Figure 4d). Despite the flap flexibility in canagliflozin−HIV-1 PR, the protein retained an overall stable structure upon binding with either aliskiren or canagliflozin. Particularly, the active site residues appeared very stable in both complexes. Renin residues were equally flexible when the protease was bound to either darunavir or canagliflozin with fluctuations ranging from 0.5 Å to 1.5 Å (Figure 4c), although specific regions of renin varied in flexibility: Glu277 and Ala49 appeared increasingly flexible when renin was bound to canagliflozin and darunavir, respectively. However, the most important regions such as the active site and the flap of renin were very stable in both complexes.

Hydrogen Bonding Analysis. The next step toward the investigation of enhanced binding modes between the inhibitors and the proteases was the identification of HB interactions that stabilize the complexes. Dominant hydrogen bonds involving the three ligands bound to the proteases are shown in Figure 5. Interactions (as % occurrence during the simulation time) are presented in Table 1. The structural investigation performed above was well complemented by the HB calculations as there was additional support on the effective

dx.doi.org/10.1021/jm300180r | J. Med. Chem. 2012, 55, 5784−5796

Table 1. Occurrence of Hydrogen Bonds between HIV-1/Renin Proteases and Canagliflozin, Aliskiren, and Darunavir[a]

HIV-1 PR Complexes		
residues in H-bonds	canagliflozin	aliskiren
Gly49	35.17	
Pro79′	13.63	
Arg6′	13.74	10.15
Gly48		94.46/66.92/10.06[b]
Asp29		52.70/47.18/44.46/42.01/27.52[b]
Renin Complexes		
residues in H-bonds	canagliflozin	darunavir
Thr77	80.98/36.68/23.98[b]	78.80
Gly217	43.44	41.67
Ser219	12.70	
Asp215		45.54/19.46/11.00[b]

[a]Occurrence is defined as the percentage of simulation time that a specific interaction exists; interactions occurring less than 10% of the simulation are not shown. [b]Multiple hydrogen bonds are formed between different atoms of the inhibitor and the specific residue.

binding of aliskiren to HIV-1 PR. From Table 1, it can be concluded that aliskiren formed permanent HB with flap residues (Gly48) and residues near the active site, such as Asp29. This is in agreement with interactions observed for darunavir in HIV-1 PR, thus suggesting an analogous binding mode.[35] The role of a water molecule to mediate the two flaps of the protease via HB interactions was of further support regarding effective aliskiren binding (Figure 5c): previous studies have denoted the importance of a water molecule to induce a stable structure of the HIV-1 PR flaps that lead to effective substrate binding into HIV-1 PR.[72] In the darunavir–renin complex, darunavir appeared to interact frequently with the pocket-covering loop of renin (Thr77), as well as with the active site residues Asp215 and Gly217. Therefore, it was suggested that darunavir is also involved in significant HB interactions that may lead to effective binding since similar interactions have been observed between aliskiren and renin.[19] The HB between darunavir and Asp215 lasted approximately for the first 10 ns and was eventually replaced by an interaction involving the drug and Gly217. This HB rearrangement has probably accounted for the structural change of renin's binding cavity mentioned above. Finally, canagliflozin participated in extended HB networks when bound to either renin or HIV-1 PR, with similar interactions to darunavir and aliskiren complexes. Its constant interaction with the Thr77-loop residue along with a less frequent interaction with active site residues (Gly217 and Ser219) stabilized the complex of renin in a tight conformation. It is worth noting that the great stability of Gly217 mentioned in the structural analysis previously was well justified by its involvement in HB with canagliflozin. Also, the canagliflozin–HIV-1 PR complex, even though it lacks significant interactions involving active site residues, presented hydrogen bonds between canagliflozin and flap residue Gly49, Pro79′, and Arg6′.

While renin complexes with darunavir and canagliflozin involved active site residues (Asp215 and Gly217) in direct interactions with the ligand, it was interesting to observe that all HIV-1 PR complexes showed hydrogen bonds between ligands and non-active site residues, with the exception of aliskiren–HIV-1 PR, where the drug was associated with the (near-active site) residue Asp29. This is consistent with previous observations on several PIs bound to HIV-1 PR that relate strong binding effects with enhanced backbone interactions between drugs and close to the active site (or flaps) protease residues, not necessarily with the catalytic triplet.[73]

Positional variations for the side chains of residues directly interacting with the ligands have been estimated by atomic fluctuation calculations. It was interesting to observe that side chain atoms in all complexes appeared relatively stable with fluctuations <1.5 Å, comparable to the very stable side chains of the catalytic residues (Table S3, Supporting Information).

Since it was suggested that darunavir participates in significant interactions with renin leading to a strong binding effect, the possibility of renin inhibition via similar interactions by other PIs naturally arises. First-generation HIV-1 PR inhibitors (saquinavir, ritonavir, indinavir, and nelfinavir; Table S2, Supporting Information) are peptide-like PIs with large hydrophobic groups.[73] High affinity for HIV-1 PR is

Table 2. Contributions to the Binding Free Energy (ΔG_{bind}) for Proteases' Complexes Computed with the MM–PBSA Method[a]

	HIV-1 PR		renin	
energetic analysis	aliskiren	canagliflozin	darunavir	canagliflozin
ΔE_{elec}	−32.16 ± 0.09[b]	−30.57 ± 0.08	−29.23 ± 0.10	−31.76 ± 0.08
ΔE_{vdW}	−55.75 ± 0.08	−37.13 ± 0.08	−34.47 ± 0.08	−45.63 ± 0.07
ΔE_{MM}	−87.91 ± 0.08	−67.70 ± 0.06	−63.70 ± 0.07	−77.93 ± 0.07
ΔG_{NP}	−8.59 ± 0.07	−6.35 ± 0.09	−3.62 ± 0.06	−1.07 ± 0.09
ΔG_{PB}	58.95 ± 0.09	40.08 ± 0.11	37.53 ± 0.11	51.54 ± 0.09
ΔG_{sol}	50.36 ± 0.09	33.73 ± 0.09	35.15 ± 0.08	50.47 ± 0.09
$\Delta G_{elec(tot)}$	26.79 ± 0.08	9.51 ± 0.06	8.30 ± 0.07	19.78 ± 0.08
ΔH	−37.55 ± 0.09	−33.97 ± 0.09	−28.55 ± 0.09	−27.46 ± 0.09
$-T\Delta S$	28.11 ± 0.29	24.50 ± 0.24	19.72 ± 0.27	18.34 ± 0.29
ΔG_{bind}	−9.44 ± 0.30	−9.47 ± 0.39	−8.83 ± 0.30	−9.12 ± 0.33
$\Delta G_{docking}$[c]	−10.12	−10.91	−11.01	−10.34
K_i	76.5[d]	628[d]	261[e]	159[e]
ΔG_{exp}[f]	−9.55	−8.32		

[a]Experimental K_i values and docking results are also presented. Units in kcal/mol; MM–PBSA analysis is based on the last 10 ns of the simulation. [b]Standard error (SE) values: SE = standard deviation/$N^{1/2}$, where N is the number of trajectory snapshots used in MM–PBSA calculations (N = 100 for entropy/ΔG_{bind} calculations, N = 1250 for everything else). [c]$\Delta G_{docking}$ has been calculated with DOCK6. [d]Experimental K_i values in nM. [e]Predicted K_i values in nM, calculated at 293.15 K. [f]ΔG_{exp} has been calculated from experimental K_i values at 293.15 K via $\Delta G_{exp} = RT\ln K_i$.

dx.doi.org/10.1021/jm300180r | J. Med. Chem. 2012, 55, 5784–5796

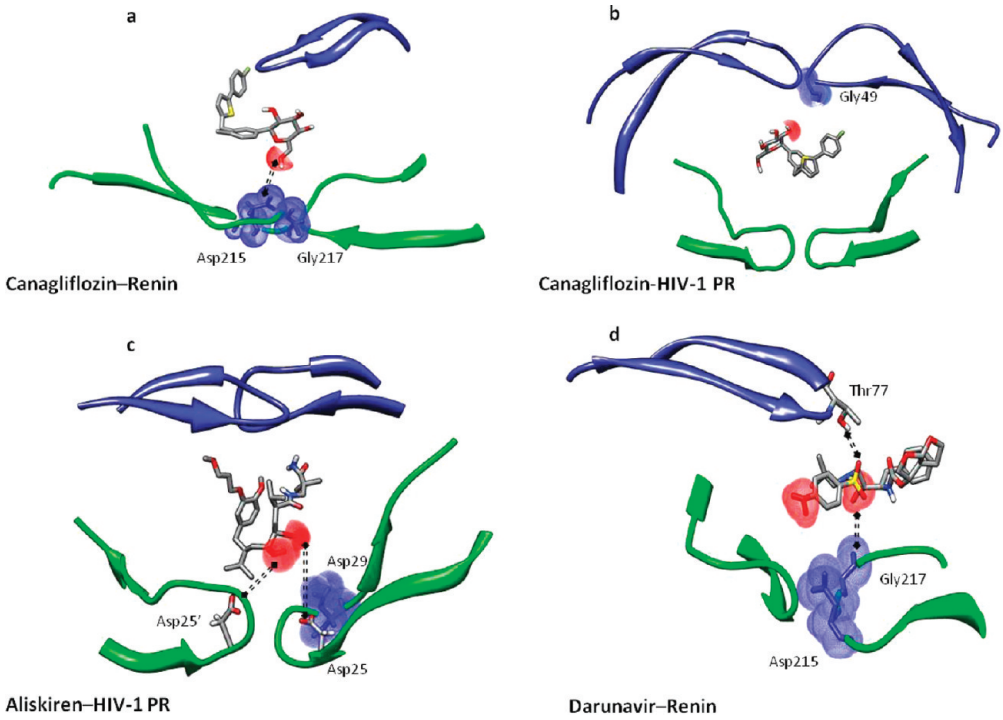

Figure 6. Significant electrostatic interactions (double dotted lines) and van der Waals contacts formed between ligands (red areas) and critical residues of the proteases (blue areas).

achieved via interactions such as hydrogen bonds between the drugs and the backbone of the protease as well as via hydrophobic contacts. Moreover, these inhibitors possess a central hydroxyl group that interacts with the active site. Since this HB interaction also exists between darunavir and renin (Figure 4d), it is reasonable to deduce that other PIs may also inhibit renin. Second-generation inhibitors, such as lopinavir, atazanavir, (fos)amprenavir, and tipranavir (Table S2, Supporting Information) may have even more profound effects on renin inhibition since they resemble darunavir more. Indeed, these PIs were designed to have reduced peptidic characteristics by replacing a carbonyl group with a sulfonamide group (amprenavir, tipranavir) to overcome several shortcomings of the previous inhibitors. Also, tetrahydrofuran (THF) and bis-tetrahydrofuran (bis-THF) groups were added to amprenavir and darunavir, respectively, to introduce nonpeptidic HB candidates. Especially, amprenavir may induce very "darunavir-like" interactions in renin since it also possesses an amino phenyl moiety that in the case of darunavir forms two hydrogen bonds with Asp215 of renin (Figure 4d). To summarize, the presence of a hydroxyl group in all PIs, along with the sulfonamide group in amprenavir and tipranavir and the amino phenyl moiety in amprenavir render these PIs possible candidates for renin inhibition too.

Inhibition Assays and MM–PBSA Analysis. To estimate the energetic contributions of binding in a reliable and detailed fashion, the MM–PBSA method has been applied to the four complexes. Convergence has been achieved for each system almost after 8 ns from the beginning of the simulations (Figure S4, Supporting Information); therefore, we chose to report calculations on the last 10 ns of each trajectory. The MM–PBSA results are summarized in Table 2. The binding energy calculations rationalized our previous findings as all three compounds presented adequate binding to HIV-1 PR and renin. More specifically, darunavir was implicated in less efficient binding when associated with renin (ΔG_{bind} = −8.8 kcal mol^{-1}) than when aliskiren is associated with HIV-1 PR (ΔG_{bind} = −9.4 kcal mol^{-1}). Following the previous structural analysis, this was something to be expected since structural rearrangements in aliskiren–HIV-1 PR were slightly less profound than the corresponding changes in darunavir–renin. Additionally, HB analysis supported such an observation as aliskiren was involved in more HB interactions when bound to HIV-1 PR (the role of water to bridge the flaps may also be important) than darunavir when bound to renin (Table 1). It is also important to note that canagliflozin presented relatively high affinity to both proteins as is reflected by the free energies of binding for its complexes: ΔG_{bind} = −9.5 kcal mol^{-1} and ΔG_{bind} = −9.1 kcal mol^{-1} for HIV-1 PR and renin, respectively. Despite indications for greater structural stability of canagliflozin–renin instead of canagliflozin–HIV-1 PR, the binding free energy calculations implicated canagliflozin as a potential, dual inhibitor of the proteases. Energy decomposition to individual contributions revealed that van der Waals and electrostatics act most favorably toward effective binding for all complexes. The nonpolar contribution to solvation further contributes to the total binding energy.

Finally, energy partition for individual residues of the proteases has been attempted to identify the source of principal contributions to the total binding energy. The majority of them belong to either the binding cavity or the flap region of each protease (Figure S5, Supporting Information). Interestingly, active site residues of HIV-1 PR and renin contribute significantly to the binding energy of both canagliflozin–protease complexes, thus implicating that interactions between canagliflozin and the active site acted very effectively toward binding. Similarly, Ile50 further enhanced binding, despite the increased flexibility of the flap in the canagliflozin–HIV-1 PR complex. Darunavir in renin as well as aliskiren in HIV-1 PR displayed analogous behavior, as the active site residues

dx.doi.org/10.1021/jm300180r | J. Med. Chem. 2012, 55, 5784–5796

presented high contributions. Additional pairwise energy decomposition revealed the main energy contributions between each ligand and the proteases (Table S4, Supporting Information). The van der Waals contacts and electrostatic interactions that contribute most to the total binding energy in the four complexes are highlighted in Figure 6. It was observed that active site residues of renin (Asp215 and Gly217) present enhanced van der Waals and electrostatic interactions with both canagliflozin and darunavir. Also, the Gly49 flap residue and Asp29 of HIV-1 PR formed favorable van der Waals interactions with canagliflozin and aliskiren, respectively. It is interesting to note that in the canagliflozin−renin complex despite the fact that Asp215 is not involved in hydrogen bonds with the ligand, it participates in strong van der Waals and electrostatic interactions. Similarly, in aliskiren−HIV-1 PR the electrostatics between the active site Asp25/25′ and the drug contribute favorably to binding.

Inhibition assays to aliskiren−HIV-1 PR and canagliflozin−HIV-1 PR complexes further supported our MM−PBSA calculations: undoubtedly, aliskiren appeared to be an effective HIV-1 PR inhibitor (K_i = 76.5 ± 5 nM, ΔG_{bind} = −9.6 kcal mol^{-1} at 293 K), in agreement with our results (percent error between experiment and prediction = 1.2%) even if it is less effective than darunavir (Table 2). Canagliflozin also presented adequate inhibitory action, with K_i = 628 ± 16 nM and ΔG_{bind} = −8.3 kcal mol^{-1}, approximately 1 kcal mol^{-1} higher than the MM−PBSA predicted value. A plausible explanation for this difference may be attributed to the scaffold of canagliflozin that may prevent the extensive formation of hydrogen bonds with HIV-1 PR, in contrast to aliskiren (Table 1). MM−PBSA calculations for darunavir−HIV-1 PR showed a strong inhibitory effect as expected (K_i = 2.86 nM, ΔG_{bind}= −11.46 kcal/mol), in agreement with inhibition assay's values (K_i = 0.5 nM, ΔG_{bind}= −12.48 kcal/mol). The MM−PBSA results reasonably reproduce the experimental data, with a linear correlation coefficient (r^2) of 0.92 for the complexes of HIV-1 PR with the three inhibitors and of renin with aliskiren (Figure S6).

Implications on Dual Inhibition of Additional Aspartic Proteases and SGLT2. In an attempt to further validate our findings by generalizing the dual inhibition of aspartic proteases, we have also considered five additional members of the family [pepsin, β-secretase 1 (BACE-1), human T-cell leukemia virus protease (HTLV-1), plasmepsin 2, and memapsin 2][73] to perform docking calculations with darunavir and aliskiren. Docking results indicated that both compounds inhibit the proteases, in support of a hypothesis of non-specificity among the members of the family (Table S5, Supporting Information). Particularly, BACE-1, plasmepsin 2 and memapsin 2 were inhibited by each compound with similar strength as HIV-1 PR and renin did. However, it was observed that renin-like proteins, such as pepsin and BACE-1 are more profoundly inhibited by aliskiren than darunavir, while HTLV-1 which resembles HIV-1 PR has a stronger inhibitory effect upon darunavir binding than aliskiren. Although most of the aspartic proteases, such as HIV-1 PR and memapsin 2, have a broad specificity, it has been indicated that few proteins involved in the regulation of physiological processes (e.g., renin, pepsin) present a highly narrow specificity that hinders the development of potent inhibitors.[73] Our study partially justified the aforementioned statement (especially in the case of pepsin, which appeared highly specific toward aliskiren binding), and it was interesting to observe the nonspecificity of darunavir and aliskiren against the other members of the family. Significantly, the nonspecificity of the two drugs was also apparent in the case of renin, which is characterized by very high specificity. It has been suggested that the flexibility of the binding pockets of aspartic proteases determines the specificity, with a broad specificity to accompany the reshaping of binding cavities in response to different ligands.[73] Such substrate-specificity studies, along with the targeting of structurally conserved and backbone regions of the protease, may lead to the design of potent inhibitors. For example, memapsin 2 possesses a relatively extended substrate binding-site; therefore, effective drug design should focus on a well-filling inhibitor to achieve potency and specificity. Future drug design may be guided by the search for candidate inhibitors that match the specificity pockets of the protease in terms of their shape, charge, hydrophobicity, and HB interactions.

SGLT2 is a transmembrane protein involved in Na^+/glucose transport. As predicted by experimental and *in silico* studies, vibrio SGLT (no human SGLT2 crystal structure has been reported to date) has 14 membrane-spanning helices with extracellular amino and carboxy termini. vSGLT binds galactose into a channel consisting of residues such as Trp264, Lys294, Tyr87, Glu88, Ser91, Tyr69, Glu87, and Asn260. The channel of vSGLT bears no similarity with the catalytic site of either HIV-1 PR or renin. We have also performed docking calculations for two vSGLT complexes, after replacing galactose from the crystal structure with aliskiren/darunavir. Binding energies of −6.4 and −6.2 kcal/mol for aliskiren and darunavir, respectively, were estimated. Therefore, despite the absence of a catalytic Asp-Thr-Gly sequence, a weak inhibitory effect may be observed in the case of vSGLT.

CONCLUSIONS

Two aspartic proteases, HIV-1 PR and renin, possessing several structural characteristics in common have been compared regarding their mode of action and conformational properties upon binding. Molecular docking calculations suggested that canagliflozin, an antidiabetic, SGLT2 inhibitor may be also an efficient inhibitor for both proteases. Additionally, darunavir and aliskiren, two potent drugs associated with HIV-1 PR and renin, respectively, were exchanged between proteases to investigate whether the structural similarities of the proteases result in similar conformational changes upon binding to the same inhibitor. Twenty nanosecond MD simulations for the four complexes (canagliflozin−HIV-1 PR, canagliflozin−renin, darunavir−renin, and aliskiren−HIV-1 PR) have been performed to observe the stabilization of all structures into inhibitor-bound conformations with reduced flexibility. Canagliflozin induced structural changes that accompany binding to both proteins. The darunavir−renin complex resulted in a stable structure and presented a strong hydrogen bonding network involving the drug and mainly loop residue Thr77 and active site residues Asp215 and Gly217. Similarly, the aliskiren−HIV-1 PR complex was involved in frequent HB interactions between aliskiren and flap residues (Gly48), as well as with active site residues (Asp29). Furthermore, a water molecule bridged the flaps of the protease via hydrogen bonds. These findings implicated canagliflozin, aliskiren, and darunavir as effective, dual inhibitors of both protein systems.

Additionally, MM−PBSA free energy calculations described the binding modes of HIV-1 PR and renin in a quantitative way. The total free energy of binding for all complexes was predicted to be adequate, with canagliflozin serving as a very effective dual

inhibitor (ΔG_{bind} = −9.5 kcal mol^{-1} and ΔG_{bind} = −9.1 kcal mol^{-1} for canagliflozin−HIV-1 PR and canagliflozin−renin, respectively). This finding is of paramount importance since it is well-known that AIDS patients who follow traditional therapy eventually develop diabetes. Thus, canagliflozin-based drug design may lead to the elimination of this problem. Darunavir−renin and aliskiren−HIV-1 PR binding energies were calculated to be −8.8 kcal mol^{-1} and −9.4 kcal mol^{-1}, respectively. The most favorable contributions to the binding energy were mainly due to van der Waals and electrostatic interactions involving active site and flap residues. Importantly, experimental confirmation of our calculations has been offered by inhibition assays for canagliflozin−HIV-1 PR and aliskiren−HIV-1 PR complexes. Finally, the interaction between aliskiren and DMPC bilayer was investigated through long MD simulations to reveal that the drug was accommodated in the interior of the bilayer, in an S-shaped conformation, which was stabilized via HB interactions with the lipids and water molecules (see Supporting Information). This suggested also the ability of similar compounds to penetrate the bilayer, a finding of direct biological significance.

This study strongly suggested that particular drugs currently used for the treatment of AIDS, hypertension, and diabetes could serve as dual inhibitors of HIV-1 PR and renin. Examples include the aliskiren-related hypertension treatment that may also help against AIDS and the use of canagliflozin to induce pronounced effects toward proteases' inhibition. Importantly, since the development of diabetes is associated with AIDS and hypertension, the design of new HIV-1 PR and renin inhibitors based on antidiabetic drug scaffolds would be particularly beneficial.

■ ASSOCIATED CONTENT

Supporting Information

Figures showing the rmsd of the apo form of renin, active site−flap distances for all complexes, rmsd for darunavir and aliskiren inside renin and HIV−1 PR, MM−PBSA results, per residue decomposition for all complexes, correlation between experimental and predicted energies, and the DMPC molecule; tables showing binding energies for test compounds, binding energies for commercial HIV-1 PR and renin inhibitors, fluctuations for selected side chain atoms, pairwise energy decomposition between ligands and selected residues of the proteases, and docking results for aliskiren and darunavir into five additional aspartic proteases; and summary of aliskiren−DMPC MD results. This material is available free of charge via the Internet at http://pubs.acs.org.

■ AUTHOR INFORMATION

Corresponding Author

*(G.L.) Tel: +30-210-727-3894. E-mail: gleonis@eie.gr. (M.G.P.) Tel: +30-210-727-3892. E-mail: mpapad@eie.gr.

Notes

The authors declare no competing financial interest.

■ ACKNOWLEDGMENTS

This research has been cofinanced by the European Union (European Social Fund−ESF) and Greek national funds through the Operational Program "Education and Lifelong Learning" of the National Strategic Reference Framework (NSRF)−Research Funding Program: Heracleitus II, investing in knowledge society through the European Social Fund. Funding provided by the European Commission for the FP7-REGPOT-2009-1 Project 'ARCADE' (Grant Agreement No. 245866) is also acknowledged.

■ ABBREVIATIONS USED

MM−PBSA, molecular mechanics Poisson−Boltzmann surface area; SGLT, sodium glucose cotransporter; HAART, highly active antiretroviral therapy; PI, protease inhibitor

■ REFERENCES

(1) Source available at http://www.unaids.org/.

(2) Kearney, P. M.; Whelton, M.; Reynolds, K.; Muntner, P.; Whelton, P. K.; He, J. Global burden of hypertension: analysis of worldwide data. *Lancet* **2005**, *365*, 217−223.

(3) Brik, A.; Wong, C. H. HIV-1 protease: mechanism and drug discovery. *Org. Biomol. Chem.* **2003**, *1*, 5−14.

(4) Tice, C. M. Renin inhibitors. *Annu. Rep. Med. Chem.* **2006**, *41*, 155−167.

(5) Paul, M.; Poyan Mehr, A.; Kreutz, R. Physiology of local renin-angiotensin systems. *Physiol Rev.* **2006**, *86*, 747−803.

(6) Wood, J. M.; Stanton, J. L.; Hofbauer, K. G. Inhibitors of renin as potential therapeutic agents. *J. Enzyme Inhib.* **1987**, *1*, 169−185.

(7) Powell, N. A.; Ciske, F. L.; Cai, C.; Holsworth, D. D.; Mennen, K.; Van Huis, C. A.; Jalaie, M.; Day, J.; Mastronardi, M.; McConnell, P.; Mochalkin, I.; Zhang, E.; Ryan, M. J.; Bryant, J.; Collard, W.; Ferreira, S.; Gu, C.; Collins, R.; Edmunds, J. J. Rational design of 6-(2,4-diaminopyrimidinyl)-1,4-benzoxazin-3-ones as small molecule renin inhibitors. *Bioorg. Med. Chem.* **2007**, *15*, 5912−5949.

(8) Coates, L.; Tuan, H.-F.; Tomanicek, S.; Kovalevsky, A.; Mustyakimov, M.; Erskine, P.; Cooper, J. The catalytic mechanism of an aspartic proteinase explored with neutron and X-ray diffraction. *J. Am. Chem. Soc.* **2008**, *130*, 7235−7237.

(9) Freedberg, D. I.; Ishima, R.; Jacob, J.; Wang, Y. X.; Kustanovich, I.; Louis, J. M.; Torchia, D. A. Rapid structural fluctuations of the free HIV protease flaps in solution: Relationship to crystal structures and comparison with predictions of dynamics calculations. *Protein Sci.* **2002**, *11*, 221−232.

(10) (a) Hornak, V.; Okur, A.; Rizzo, R. C.; Simmerling, C. HIV-1 protease flaps spontaneously open and reclose in molecular dynamics simulations. *Proc. Natl. Acad. Sci. U.S.A.* **2006**, *103*, 915−920. (b) Hornak, V.; Okur, A.; Rizzo, R. C.; Simmerling, C. HIV-1 protease flaps spontaneously close to the correct structure in simulations following manual placement of an inhibitor into the open state. *J. Am. Chem. Soc.* **2006**, *128* (9), 2812−2813.

(11) Nicholson, L. K.; Yamazaki, T.; Torchia, D. A.; Grzesiek, S.; Bax, A.; Stahl, S. J.; Kaufman, J. D.; Wingfield, P. T.; Lam, P. Y.; Jadhav, P. K. Flexibility and function in HIV-1 protease. *Nat. Struct. Biol.* **1995**, *2*, 274−280.

(12) Rahuel, J.; Priestle, P.; Grutter, M. G. The crystal structures of recombinant glycosylated human renin alone and in complex with a transition state analog inhibitor. *J. Struct. Biol.* **1991**, *107*, 227−236.

(13) Jensen, C.; Herold, P.; Brunner, H. R. Aliskiren: the first renin inhibitor for clinical treatment. *Nat. Rev. Drug Discovery* **2008**, *7*, 399−410.

(14) Sharma, K. S.; Evans, D. B.; Hui, J. O.; Henrikson, R. L. Could angiotensin i be produced from a renin substrate by the HIV-I protease? *Anal. Biochem.* **1991**, *198*, 363−367.

(15) Zhang, Z. Y.; Reardon, I. M.; Hui, J. O.; O'Connell, K. L.; Poorman, R. A.; Tomasselli, A. G.; Heinrikson, R. L. Zinc inhibition of renin and the protease from human immunodeficiency virus type I. *Biochemistry* **1991**, *30* (36), 8717−8721.

(16) Vondrasek, J.; Wlodawer, A. HIVdb: a database of the structures of human immunodeficiency virus protease. *Proteins* **2002**, *49*, 429−431.

(17) Lapatto, R.; Blundell, T.; Hemmings, A.; Overington, J.; Wilderspin, A.; Wood, S.; Merson, J. R.; Whittle, P. J.; Danley, D. E.; Geoghegan, K. F. X-ray analysis of HIV-1 proteinase at 2.7 Å

resolution confirms structural homology among retroviral enzymes. *Nature* **1989**, *342*, 299−302.
(18) Navia, M. A.; Fitzgerald, P. M.; McKeever, B. M.; Leu, C. T.; Heimbach, J. C.; Herber, W. K.; Sigal, I. S.; Darke, P. L.; Springer, J. P. Three-dimensional structure of aspartyl protease from human immunodeficiency virus HIV-1. *Nature* **1989**, *337*, 615−620.
(19) Politi, A.; Leonis, G.; Tzoupis, H.; Ntountaniotis, D.; Papadopoulos, M. G.; Golic Grdadolnik, S.; Mavromoustakos, T. Conformational properties and energetic analysis of aliskiren in solution and receptor site. *Mol. Inf.* **2011**, *30*, 973−985.
(20) Scheiper, B.; Matter, H.; Steinhagen, H.; Stilz, U.; Böcskei, Z.; Fleury, V.; McCort, G. Discovery and optimization of a new class of potent and non-chiral indole-3-carboxamide-based renin inhibitors. *Bioorg. Med. Chem. Lett.* **2010**, *20*, 6268−6272.
(21) Tokarski, J. S.; Hopfinger, A. J. Prediction of ligand-receptor binding thermodynamics by free energy force field (FEFF) 3D-QSAR analysis: application to a set of peptidometic renin inhibitors. *J. Chem. Inf. Comput. Sci.* **1997**, *37*, 779−791.
(22) Hou, T.; McLaughlin, W. A.; Wang, W. Evaluating the potency of HIV-1 protease drugs to combat resistance. *Proteins* **2008**, *71*, 1163−1174.
(23) Hyland, L. J.; Tomaszek, T. A., Jr.; Meek, T. D. Human immunodeficiency virus-1 protease. 2. Use of pH rate studies and solvent kinetic isotope effects to elucidate details of chemical mechanism. *Biochemistry* **1991**, *30*, 8454−8463.
(24) Pietrucci, F.; Marinelli, F.; Carloni, P.; Laio, A. Substrate binding mechanism of HIV-1 protease from explicit-solvent atomistic simulations. *J. Am. Chem. Soc.* **2009**, *131*, 11811−11818.
(25) Tzoupis, H.; Leonis, G.; Durdagi, S.; Mouchlis, V.; Mavromoustakos, T.; Papadopoulos, M. G. Binding of novel fullerene inhibitors to HIV-1 protease: insight through molecular dynamics and molecular mechanics Poisson−Boltzmann surface area calculations. *J. Comput.-Aided Mol. Des.* **2011**, *25*, 959−976.
(26) Smith, A. B., III; Hirschmann, R.; Pasternak, A.; Akaishi, R.; Guzman, M. C.; Jones, D. R.; Keenan, T. P.; Sprengeler, P. A. Design and synthesis of peptidomimetic inhibitors of HIV-1 protease and renin. Evidence for improved transport. *J. Med. Chem.* **1994**, *37* (2), 215−218.
(27) *Diabetes Pipeline: Intense Activity to Meet Unmet Need*; InsightPharma: Langhorne, PA, 2010; p. vii.http://www.insightpharmareports.com/uploadedFiles/ExecutiveSummary.pdf.; http://clinicaltrials.gov/ct2/show/NCT01064414.
(28) Zhou, H.; Danger, D. P.; Dock, S. T.; Hawley, L.; Roller, S. G.; Smith, C. D.; Handlon, A. L. Synthesis and SAR of Benzisothiazole- and Indolizine-β-D-glucopyranoside Inhibitors of SGLT2. *ACS Med. Chem. Lett.* **2010**, *1*, 19−23.
(29) Goodwin, N. C.; Mabon, R.; Harrison, B. A.; Shadoan, M. K.; Almstead, Z. Y.; Xie, Y.; Healy, J.; Buhring, L. M.; DaCosta, C. M.; Bardenhagen, J.; Mseeh, F.; Liu, Q.; Nouraldeen, A.; Wilson, A. G. E.; Kimball, S. D.; Powell, D. R.; Rawlins, D. B. Novel L-xylose derivatives as selective sodium-dependent glucose cotransporter 2 (SGLT2) inhibitors for the treatment of type 2 diabetes. *J. Med. Chem.* **2009**, *52*, 6201−6204.
(30) De Meyer, S.; Azijn, H.; Surleraux, D.; Jochmans, D.; Tahri, A.; Pauwels, R.; Wigerinck, P.; de Bethune, M. P. TMC114, a novel HIV-1 protease inhibitor active against protease inhibitor-resistant viruses, including a broad range of clinical isolates. *Antimicrob. Agents Chemother.* **2005**, *49*, 2314−2321.
(31) Koh, Y.; Nakata, H.; Maeda, K.; Ogata, H.; Bilcer, G.; Devasamudram, T.; Kincaid, J. F.; Boross, P.; Wang, Y. F.; Tie, Y.; Volarath, P.; Gaddis, L.; Harrison, R. W.; Weber, I. T.; Ghosh, A. K.; Mitsuya, H. Novel bis-tetrahydrofuranylurethane-containing non-peptidic protease inhibitor (PI) UIC-94017 (TMC114) with potent activity against multi-PI-resistant human immunodeficiency virus in vitro. *Antimicrob. Agents Chemother.* **2003**, *47*, 3123−3129.
(32) Kovalevsky, A. Y.; Liu, F.; Leshchenko, S.; Ghosh, A. K.; Louis, J. M.; Harrison, R. W.; Weber, I. T. Ultra-high resolution crystal structure of HIV-1 protease mutant reveals two binding sites for clinical inhibitor TMC114. *J. Mol. Biol.* **2006**, *363*, 161−173.
(33) Lefebvre, E.; Schiffer, C. A. Resilience to resistance of HIV-1 protease inhibitors: profile of darunavir. *AIDS Rev.* **2008**, *10*, 131−142.
(34) Tie, Y.; Boross, P. I.; Wang, Y. F.; Gaddis, L.; Hussain, A. K.; Leshchenko, S.; Ghosh, A. K.; Louis, J. M.; Harrison, R. W.; Weber, I. T. High resolution crystal structures of HIV-1 protease with a potent non-peptide inhibitor (UIC-94017) active against multidrug-resistant clinical strains. *J. Mol. Biol.* **2004**, *338*, 341−352.
(35) Ghosh, A. K.; Chapsal, B. D.; Weber, I. T.; Mitsuya, H. Design of protease inhibitors targeting protein backbone: an effective strategy for combating drug resistance. *Acc. Chem. Res.* **2008**, *41*, 78−86.
(36) Wood, J. M.; Maibaum, J.; Rahuel, J.; Grütter, M. G.; Cohen, N. C.; Rasetti, V.; Rüger, H.; Göschke, R.; Stutz, S.; Fuhrer, W.; Schilling, W.; Rigollier, P.; Yamaguchi, Y.; Cumin, F.; Baum, H. P.; Schnell, C. R.; Herold, P.; Mah, R.; Jensen, C.; O'Brien, E.; Stanton, A.; Bedigian, M. P. Structure-based design of aliskiren, a novel orally effective renin inhibitor. *Biochem. Biophys. Res. Commun.* **2003**, *308* (4), 698−705.
(37) Wang, W.; Donini, O.; Reyes, C. M.; Kollman, P. A. Biomolecular simulations: recent developments in force fields, simulations of enzyme catalysis, protein−ligand, protein−protein, and protein−nucleic acid noncovalent interactions. *Annu. Rev. Biophys. Biomol. Struct.* **2001**, *30*, 211−243.
(38) Wan, S.; Coveney, P. V.; Flower, D. R. Peptide recognition by the T cell receptor: comparison of binding free energies from thermodynamic integration, Poisson−Boltzmann and linear interaction energy approximations. *Philos. Trans. R. Soc., A* **2005**, *363*, 2037−2053.
(39) Jorgensen, W. L. The Many Roles of Computation in Drug Discovery. *Science* **2004**, *303*, 1813−1818.
(40) Wang, W.; Kollman, P. A. Computational study of protein specificity: The molecular basis of HIV-1 protease drug resistance. *Proc. Natl. Acad. Sci. U.S.A.* **2001**, *98*, 14937−14942.
(41) Xu, Y.; Wang, R. A computational analysis of the binding affinities of FKBP12 inhibitors using the MM-PB/SA method. *Proteins* **2006**, *64*, 1058−1068.
(42) Gohlke, H.; Kiel, C.; Case, D. A. Insights into protein−protein binding by binding free energy calculation and free energy decomposition for the Ras-Raf and Ras-RaIGDS complexes. *J. Mol. Biol.* **2003**, *330*, 891−913.
(43) Wlodawer, A.; Vondrasek, J. Inhibitors of HIV-1 protease: a major success of structure-assisted drug design. *Annu. Rev. Biophys. Biomol. Struct.* **1998**, *27*, 249−284.
(44) Hadigan, C.; Corcoran, C.; Basgoz, N.; Davis, B.; Sax, P.; Grinspoon, S. Metformin in the treatment of HIV lipodystrophy syndrome: a randomized controlled trial. *JAMA* **2000**, *284* (4), 472−477.
(45) Jung, O.; Bickel, M.; Ditting, T.; Rickerts, V.; Welk, T.; Helm, E. B.; Staszewski, S.; Geiger, H. Hypertension in HIV-1-infected patients and its impact on renal and cardiovascular integrity. *Nephrol., Dial., Transplant.* **2004**, *19*, 2250−2258.
(46) Yoon, C.; Gulick, R. M.; Hoover, D. R.; Vaamonde, C. M.; Glesby, M. J. Case-control study of diabetes mellitus in HIV-infected patients. *JAIDS* **2004**, *37* (4), 1464−1470.
(47) Bergersen, B. M.; Sandvik, L.; Dunlop, O.; Birkeland, K.; Bruun, J. N. Prevalence of hypertension in HIV-positive patients on highly active retroviral therapy (HAART) compared with HAART-naive and HIV-negative controls: Results from a Norwegian study of 721 patients. *Eur. J. Clin. Microbiol. Infect. Dis.* **2003**, *22*, 731−736.
(48) Seaberg, E. C.; Munoz, A.; Lu, M; Detels, R; Margolick, J. B.; Riddler, S. A.; Williams, C. M.; Phair, J. P. Association between highly active antiretroviral therapy and hypertension in a large cohort of men followed from 1984 to 2003. *AIDS* **2005**, *19* (9), 953−960.
(49) Graves, A. P.; Shivakumar, D. M.; Boyce, S. E.; Jacobson, M. P.; Case, D. A.; Shoichet., D. K. Rescoring docking hit lists for model cavity sites: predictions and experimental testing. *J. Mol. Biol.* **2008**, *377*, 914−934.
(50) Wang, J.; Wang, W.; Kollman, P. A.; Case, D. A. Automatic atom type and bond type perception in molecular mechanical calculations. *J. Mol. Graphics Modell.* **2006**, *25*, 247−260.

(51) Pettersen, E. F.; Goddard, T. D.; Huang, C. C.; Couch, G. S.; Greenblatt, D. M.; Meng, E. C.; Ferrin, T. E. UCSF Chimera: a visualization system for exploratory research and analysis. *J. Comput. Chem.* **2004**, *25* (13), 1605−1612.
(52) Jakalian, A.; Bush, B. L.; Jack, D. B.; Bayly, C. I. Fast, efficient generation of high-quality atomic charges. AM1-BCC model: I. Method. *J. Comput. Chem.* **2000**, *21*, 132−146.
(53) Jakalian, A.; Jack, D. B.; Bayly, C. I. Fast, efficient generation of high-quality atomic charges. AM1-BCC model: II. Parameterization and validation. *J. Comput. Chem.* **2002**, *23*, 1623−1641.
(54) Meng, E. C.; Shoichet, B. K.; Kuntz, I. D. Automated docking with grid-based energy evaluation. *J. Comput. Chem.* **1992**, *13*, 505−524.
(55) Shoichet, B. K.; Bodian, D. L.; Kuntz, I. D. Molecular docking using shape descriptors. *J. Comput. Chem.* **1992**, *13* (3), 380−397.
(56) (a) Case, D. A.; Cheatham, T.; Darden, T.; Gohlke, H.; Luo, R.; Merz, K. M., Jr.; Onufriev, A.; Simmerling, C.; Wang, B.; Woods, R. The amber biomolecular simulation programs. *J. Comput. Chem.* **2005**, *26*, 1668−1688. (b) Case, D. A.; Darden, T. A.; Cheatham, III, T. E.; Simmerling, C. L.; Wang, J.; Duke, R. E.; Luo, R.; Walker, R. C.; Zhang, W.; Merz, K. M.; Roberts, B. P.; Wang, B.; Hayik, S.; Roitberg, A.; Seabra, G.; Kolossváry, I.; Wong, K. F.; Paesani, F.; Vanicek, J.; Liu, J.; Wu, X; Brozell, S. R.; Steinbrecher, T.; Gohlke, H.; Cai, Q.; Ye, X.; Wang, J.; Hsieh, M. J.; Cui, G.; Roe, D. R.; Mathews, D. H.; Seetin, M. G.; Sagui, C.; Babin, V.; Luchko, T.; Gusarov, S.; Kovalenko, A.; Kollman, P. A. *AMBER 11*, University of California, San Francisco, CA, 2010.
(57) RSCB Protein Databank. http://www.rcsb.org/pdb/home/home.do
(58) Hornak, V.; Abel, R.; Okur, A.; Strockbine, B.; Roitberg, A.; Simmerling, C. Comparison of multiple Amber force fields and development of improved protein backbone parameters. *Proteins* **2006**, *65* (3), 712−725.
(59) Wang, J.; Wolf, R. M.; Caldwell, J. W.; Kollman, P. A.; Case, D. A. Development and testing of a general Amber force field. *J. Comput. Chem.* **2004**, *25*, 1157−1174.
(60) Jorgensen, W. L.; Madura, J. D.; Impey, R. W.; Klein, M. L. Comparison of simple potential functions for simulationg liquid water. *J. Chem. Phys.* **1983**, *79*, 926−935.
(61) Darden, T.; York, D.; Pedersen, L. Particle mesh Ewald: an N.Log(N) method for Ewald sums in large systems. *J. Chem. Phys.* **1993**, *98*, 10089−10092.
(62) Izaguirre, J. A.; Catarello, D. P.; Wozniak, J. M.; Skeel, R. D. Langevin stabilization of molecular dynamics. *J. Chem. Phys.* **2001**, *114*, 2090−2098.
(63) Ryckaert, J.-P.; Ciccotti, G.; Berendsen, H. J. C. Numerical integration of the cartesian equations of motion of a system with constraints: Molecular dynamics of n-alkanes. *J. Comput. Phys.* **1977**, *23*, 327−341.
(64) Honig, B.; Nichols, A. Classical electrostatics in biology and chemistry. *Science* **1995**, *268*, 1144−1149.
(65) Weiser, J.; Shenkin, P. S.; Still, W. C. Approximate atomic surfaces from linear combinations of pairwise overlaps (LCPO). *J. Comput. Chem.* **1999**, *20*, 217−230.
(66) Hou, T.; Wang, J.; Li, Y.; Wang., W. Assessing the performance of the MM/PBSA and MM/GBSA methods. 1. The Accuracy of binding free energy calculations based on molecular dynamics simulations. *J. Chem. Inf. Model.* **2011**, *51*, 69−82.
(67) Charlier, L.; Nespoulous, C.; Fiorucci, S.; Antonczak, S.; Golebiowski, J. Binding free energy prediction in strongly hydrophobic biomolecular systems. *Phys. Chem. Chem. Phys.* **2007**, *9*, 5761−5771.
(68) Simmerling, C.; Elber., R.; Zhang, J. *Moil-View, A Program for Visualization of Structure and Dynamics of Biomolecules and STO, A Program for Computing Stochastic Paths*; Kluwer: The Netherlands, 1995.
(69) Weber, J.; Mesters, J. R.; Lepšík, M.; Prejdová, J.; Švec, M.; Šponarová, J.; Mlčochová, P.; Skalická, K.; Stříšovský, K.; Uhlíková, T.; Souček, M; Machala, L.; Staňková, M.; Vondrášek, J.; Klimkait, T.; Kraeusslich, H. G.; Hilgenfeld, R.; Konvalinka, J. Unusual binding mode of an HIV-1 protease inhibitor explains its potency against multi-drug-resistant virus strains. *J. Mol. Biol.* **2002**, *324*, 739−754.
(70) Williams, J. W.; Morrison, J. F. The kinetics of reversible tight-binding inhibition. *Methods Enzymol.* **1979**, *63*, 437−467.
(71) Cheng, Y.; Prusoff, W. H. Relationship between the inhibition constant (K1) and the concentration of inhibitor which causes 50% inhibition (I50) of an enzymatic reaction. *Biochem. Pharmacol.* **1973**, *22* (23), 3099−3108.
(72) Okimoto, N.; Tsukui, T.; Kitayama, K.; Hata, M.; Hoshino, T.; Tsuda, M. Molecular dynamics study of HIV-1 protease-substrate complex: Roles of the water molecules at the loop structures of the active site. *J. Am. Chem. Soc.* **2000**, *122*, 5613−5622.
(73) Ghosh, A. *Aspartic Acid Proteases as Therapeutic Targets*; John Wiley and Sons: New York, 2011.